Chemistry & Biology
Article

A *Staphylococcus aureus* Fitness Test Platform for Mechanism-Based Profiling of Antibacterial Compounds

Robert G.K. Donald,[1] Stephen Skwish,[1] R. Allyn Forsyth,[1,2] Jennifer W. Anderson,[1] Tanya Zhong,[1] Colleen Burns,[1] Suzy Lee,[1] Xin Meng,[1] Lynn LoCastro,[1] Lisa Wang Jarantow,[1] Jesus Martin,[1] Sang Ho Lee,[1] Ian Taylor,[1] David Robbins,[1,2] Cheryl Malone,[1] Liangsu Wang,[1] Carlos S. Zamudio,[1,3] Philip J. Youngman,[1] and John W. Phillips[1,*]
[1]Infectious Diseases, Merck Research Laboratories, Merck & Co., P.O. Box 2000, Rahway, NJ 07065, USA
[2]Present address: ICx Biosystems, 505 Coast Boulevard South, Suite 309, La Jolla, CA 92037, USA
[3]Present address: Semantic Laboratories, 8724-88 Villa La Jolla Drive, La Jolla, CA 92037, USA
*Correspondence: phillips.johnw@gmail.com
DOI 10.1016/j.chembiol.2009.07.004

SUMMARY

The emergence of drug-resistant bacteria coupled with the limited discovery of novel chemical scaffolds and druggable targets inspires new approaches to antibiotic development. Here we describe a chemical genomics strategy based on 245 *Staphylococcus aureus* antisense RNA strains, each engineered for reduced expression of target genes essential for *S. aureus* growth. Attenuation of gene expression can sensitize cells to compounds that inhibit the activity of a gene product or associated process. Pools of strains grown competitively in the presence of bioactive compounds generate characteristic profiles of strain sensitivities reflecting compound mechanism of action. Here, we validate this approach with a structurally and mechanistically diverse set of reference antibiotics and, in the accompanying paper in this issue of *Chemistry & Biology* (Huber et al., 2009), demonstrate its use in the discovery of new cell wall inhibitors.

INTRODUCTION

The need to develop novel antibiotics to combat emerging or established resistance to existing antibacterial therapies is universally acknowledged (Taubes, 2008). Unfortunately, the search for new antibacterial drugs remains a significant challenge (Payne et al., 2007), with only two novel therapeutics (linezolid and daptomycin) resulting from efforts spanning the last 20 years. One of the major limitations in the screening of compound libraries for antibacterials is the large number of hits coming from compounds working through a nonspecific mechanism of action (MOA). Until recently, methods that can identify antibiotics that selectively inhibit well validated or high value targets have been lacking.

Fortunately, an elegant chemical genomics strategy that allows for a quick readout of a compound's potential MOA in a living cell has emerged from the yeast research community. The approach, termed haploinsufficiency profiling (also referred to as the yeast fitness test), relies on the observation that reduction in the copy number of genes encoding particular protein targets sensitizes the cell to selective inhibitors, reducing its fitness relative to other heterozygote strains whose copy number mutations are unrelated to compound MOA (Baetz et al., 2004; Giaever et al., 1999, 2004; Lum et al., 2004). Haploinsufficiency resulting from compound treatment is quantified by microarray hybridization of amplified barcode tags, allowing inferences to be made regarding MOA. An analogous fitness test platform for the fungal pathogen *Candida albicans* (CaFT) has recently been developed and validated with a variety of well characterized antifungal compounds (Rodriguez-Suarez et al., 2007; Xu et al., 2007). The CaFT platform has been further utilized in a natural products discovery paradigm to discover a novel inhibitor of fungal poly(A) polymerase with drug-like properties that include efficacy in an animal model of disseminated candidiasis, demonstrating the practical utility of the fitness test strategy for antimicrobial drug discovery (Jiang et al., 2008).

The use of hypersensitized strains as chemical genetic tools in bacteria is feasible with regulated systems that repress essential gene expression either through the construction of conditional gene knockouts (DeVito et al., 2002) or by inducible antisense RNA (Forsyth et al., 2002; Ji et al., 2001). Such strains have been used, individually or in parallel, for the screening of synthetic or natural product compound libraries (DeVito et al., 2002; Young et al., 2006). The concept of using a pool of sensitized antisense strains in bacteria to identify compound MOA has previously been explored (Yin et al., 2004), but the full potential of this approach as a chemical genomics platform has not yet been realized. Herein we describe the first use of an integrated array of hypersensitized strains to systematically profile the MOA of small molecule antibiotics in a clinically significant pathogenic bacterium. Represented in this *S. aureus* array are 245 strains that correspond to essential genes for which xylose-inducible antisense RNA expression imparts a growth phenotype. This semiautomated system is capable of generating antisense-induced strain sensitivity (AISS) profiles reflecting the mechanistic selectivity of a structurally diverse set of reference antibiotics for a variety of known targets including the cell wall, the ribosome, nucleic acid biosynthesis, and several metabolic pathways. The platform has broad applications in the field of antibacterial drug discovery, including MOA determination for

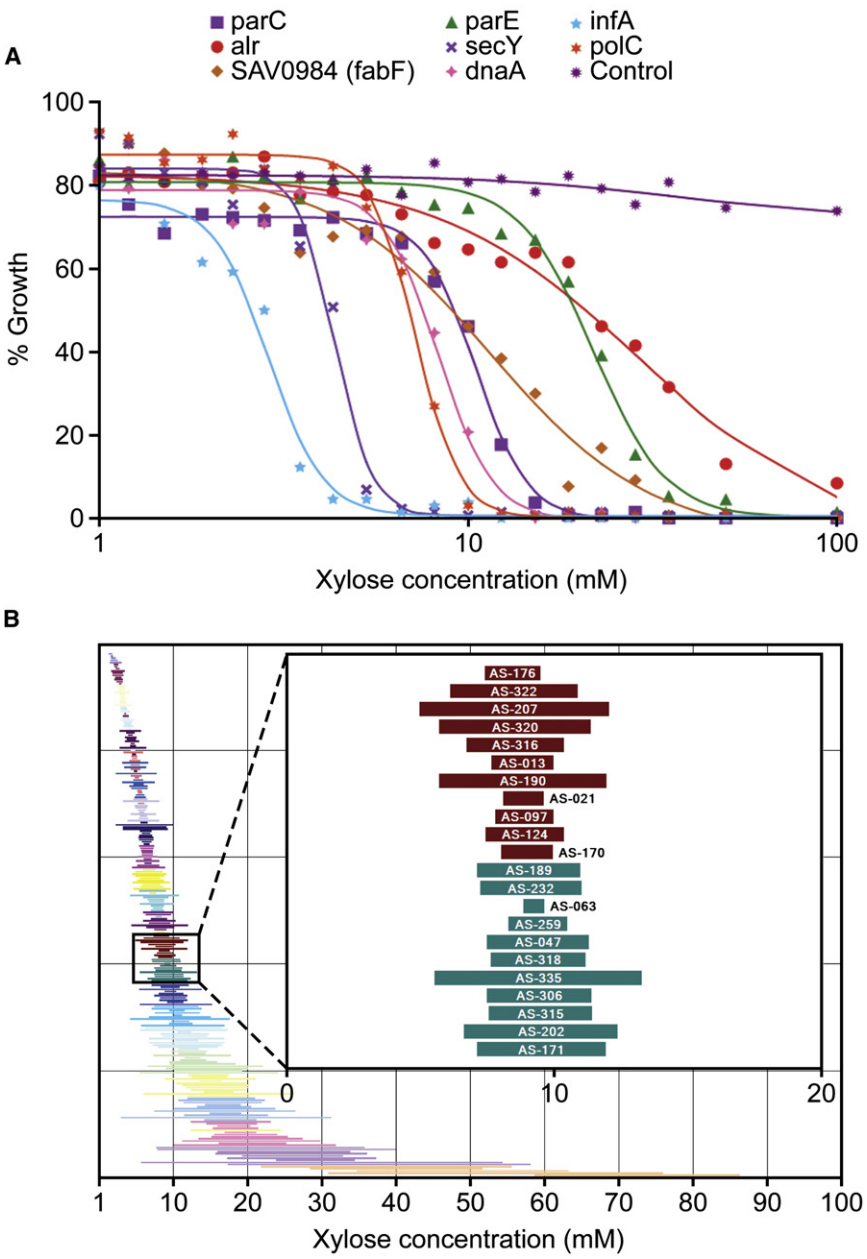

Figure 1. Binning of Antisense Strains

(A) Dose response curves for a subset of antisense strains and empty vector control strain illustrate variable sensitivity to xylose inducer.

(B) Distribution of strains into 24 bins (color coded). Data from multiple experiments were averaged (n > 3) and IC_{10} and IC_{30} values were interpolated from nonlinear regression analysis (Experimental Procedures). y axis represents the rank ordering of sensitivities from most sensitive (top) to least sensitive (bottom), based on IC_{20} values. Left and right boundaries of horizontal bars represent the xylose IC_{10} and IC_{30} values while bar length reflects the relative slope. Inset highlights bins 15 and 16.

newly discovered antibacterial agents, the identification of novel drug targets, and the detection of reporter strains whose chemically-induced hypersensitivity correlates with specific antibacterial modes of action.

RESULTS

Experimental Design

The majority of the 245 *S. aureus* antisense strains of the array (see Table S1 available online) were selected from a broader collection of 658 strains with conditional growth phenotype generated using a genome-wide shotgun cloning strategy (Forsyth et al., 2002). The array includes 30 additional strains constructed by targeted cloning to improve representation of genes known to be essential in other bacterial pathogens or that constitute validated gene targets. Represented in the array are genes involved in cell wall biosynthesis, ribosomal protein synthesis, fatty acid biosynthesis, DNA synthesis and replication, and RNA transcription. Also present are antisense strains corresponding to genes encoding glycolytic enzymes, tRNAs, tRNA-modifying enzymes, tRNA synthetases, chaperones, cell division proteins, enzymes of vitamin cofactor metabolism and oxidative phosphorylation, as well as some proteins of uncertain function. The antisense gene fragments map to 140 different operons containing between 1 and 29 open reading frames (Table S2).

In fungal systems for fitness test profiling all of the heterozygote strains can be pooled together (Giaever et al., 2004; Giaever et al., 1999; Lum et al., 2004; Xu et al., 2007) and the magnitude of the target gene depletion is fixed (at 50%). AISS profiling in *S. aureus* has the complexity of titratable levels of antisense expression and corresponding target protein depletions with strains displaying variable sensitivity to the xylose inducer (Figure 1A), which precludes combining all of the antisense strains into one pool. To achieve comparable levels of sensitivity and competitive growth, the 245 antisense strains were divided into 24 pools of 6–12 strains each that respond similarly to xylose inducer (Figure 1B). Xylose levels of individual bins varied between 1.8 and 55 mM (final concentration). To maximize strain sensitivity, we chose to perform the experiment at xylose levels that induce a modest growth defect in the antisense strains (targeted range of IC_{10}–IC_{30}), thereby establishing some biologically significant level of target protein depletion.

An overview of the AISS profiling platform that illustrates sequential microbiology, molecular biology, and data analysis steps is shown in Figure 2. The 24 bins were grown in parallel in the presence of a range of partially inhibitory concentrations

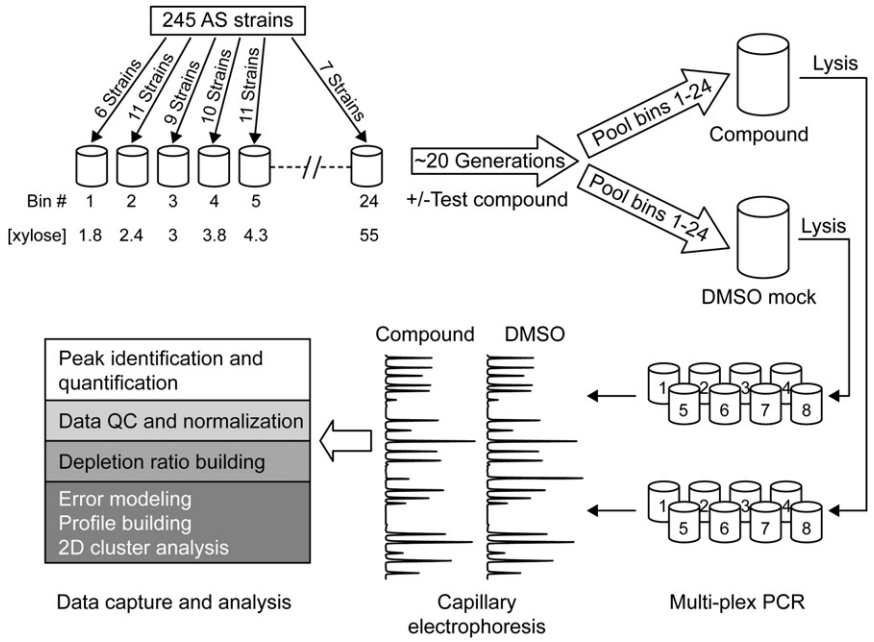

Figure 2. Generation of AISS Profiles

The 245 strains comprising the array are pooled into 24 distinct bins, with each bin assayed at a different final xylose concentration from 1.8 to 55 mM. The bins are grown for ~20 generations in the presence of test compound or 2% DMSO (mock treatment). After pooling, cells are lysed and transferred into multiplex PCR reactions for amplification with eight distinct sets of strain-specific oligonucleotide primers (termed marker sets). Approximately 30 different antisense markers are amplified per reaction, with each representing a unique antisense strain in the array. PCR products from each of the eight reactions are separated by capillary electrophoresis and identified and peak areas quantified. Captured data is then systematically quality controlled and normalized. Depletion ratios and statistical significance values are generated by comparing markers from the test compound treatment to those of the DMSO control (Experimental Procedures). AISS profiles resulting from the analysis are also subjected to higher level 2D cluster analysis (Rosetta Resolver).

of antibiotic for approximately 20 population doublings. At the end of the growth period, the relative abundances of each of the strains in the compound treatment and DMSO mock treatment groups were determined by multiplex PCR, capillary electrophoresis, and DNA fragment analysis to quantify strain-specific markers. Depletion ratios and statistical significance were generated from normalized peak area data by comparing test PCR marker abundances with mock DMSO controls (See Experimental procedures), yielding AISS profiles for each compound. Representative growth data (Figure 3A), PCR fragment analysis (Figure 3B), and the corresponding AISS profile (Figure 3C) are shown for platensimycin. In order to highlight only those strains depleting across the full range of compound concentrations presented, data were stringently filtered to show only strain depletions represented in greater than 90% of the doses. Selective depletion of the *fabF*-antisense (AS) strain in response to compound treatment is in accordance with platensimycin's well established MOA through inhibition of the FabF enzyme (Wang et al., 2006). Additional less consistently represented depletions in *accA/C*-AS (acetyl-CoA carboxylase) strains are shown in Table S3 and the unfiltered average response for the 245 strains in the array is depicted in Figure S1. To validate our approach for determining the MOAs of antibacterial compounds, we systematically profiled 59 antibacterial compounds (Table S4). Log depletion ratios and p-values were calculated for all strains for each of the qualified compound treatments (Tables S5 and S6).

Inhibitors of Enzyme Targets

Additional examples of AISS profiles of selective enzyme inhibitors are shown in Figure 4. Trimethoprim is a synthetic antifolate that inhibits dihydrofolate reductase (Burchall, 1973; Hitchings, 1973), an enzyme which regenerates reduced tetrahydrofolate for the biosynthesis of thymidylate, purines, histidine, and methionine. The associated AISS profile (Figure 4A) shows strong depletions for antisense strains corresponding to the enzymatic target dihydrofolate reductase (*dfrA*-AS) and for the enzymatically coupled thymidylate synthase (*thyA*-AS). Depletions are also observed for antisense strains associated with DNA replication: *dnlJ*-AS (DNA ligase); *recR*-AS (recombination protein); and *dnaX*-AS (polIII γ subunit). Thus, in addition to AISS profiling identifying the established target of trimethoprim, its downstream effects on DNA replication are also revealed.

Novobiocin inhibits the catalytic activity of the related heterotetrameric topoisomerase enzymes, DNA gyrase and topoismerase IV (Bellon et al., 2004; Fujimoto-Nakamura et al., 2005). Its AISS profile (Figure 4B) shows highly significant depletions in both topoisomerase IV strains *parE*-AS and *parC*-AS as well as significant depletions for the two DNA gyrase strains *gyrB*-AS and *gyrA*-AS. Thus, each of the known multimeric enzyme complexes targeted by novobiocin is faithfully resolved. Additional, less consistently represented strain depletions reflected in the novobiocin AISS profile (Table S3 and Figure S2) correspond to genes that presumably buffer the cell from the DNA damaging effects of novobiocin; these include the DNA polymerase III delta prime and α subunits (*holB*-AS and *polC*-AS, respectively) and *hu*-AS. The Hu protein is a dimeric histone-like DNA binding protein associated with DNA recombination and DNA repair (Kamashev et al., 2008).

D-cycloserine is a cell wall biosynthesis inhibitor that inhibits alanine racemase (Alr) and D-alanine-D-alanine ligase (DdlA) (Feng and Barletta, 2003; Lambert and Neuhaus, 1972). Both *alr* and *ddlA*-AS strains are strongly depleted in the D-cycloserine AISS profile (Figure 4C). Depletions of similar magnitude but lower significance are also seen for the *murF*-AS strain. The *murF* gene is cotranscribed with *ddlA* and catalyzes the addition of the carboxy terminal D-ala-D-ala dipeptide substrate provided by the cooperative functions of Alr and DdlA to sequentially assemble the peptidoglycan precursor. Therefore, AISS profiling of D-cycloserine identifies its cognate

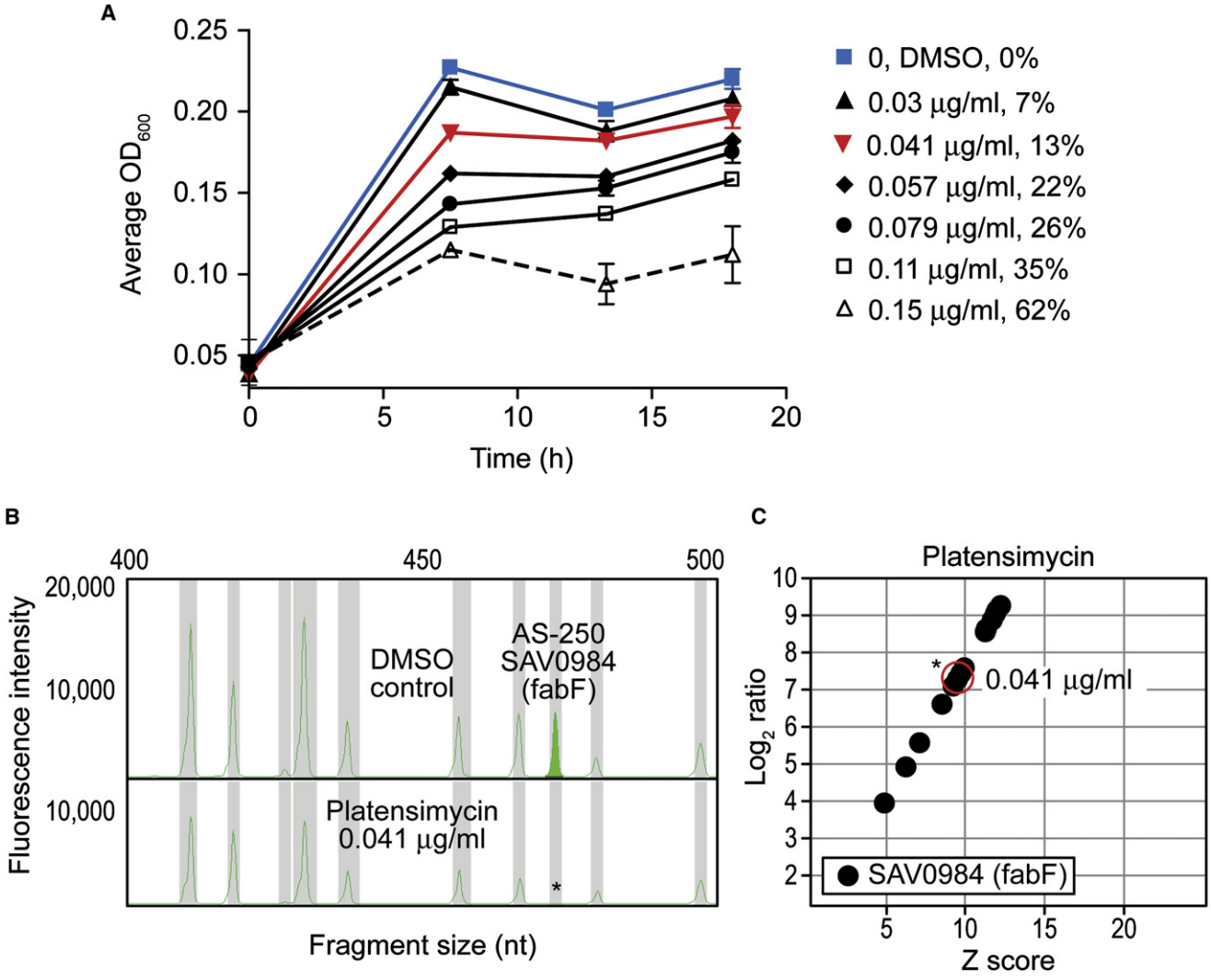

Figure 3. Profile Anatomy

(A) Growth data from a platensimycin experiment. The x axis represents time (in hours) and the y axis the growth (OD600) for the 24 bins corresponding to each treatment (mean with SD for six doses and DMSO control from two independent experiments). To attain 20 population doublings the cells are grown for three cycles with appropriate back dilutions and seeding into fresh media and drug at every cycle. Readings are taken at the end of each period (at approximately 8, 13, and 18 hr) and percentage of growth inhibition relative to the control is calculated for each compound dose at the end of the third cycle (legend). Data from the DMSO control and 0.041 µg/ml dose are highlighted in blue and red, respectively. The 0.15 µg/ml dose (62% growth inhibition; dotted line) is automatically invalidated according to QC criteria (>60% threshold).

(B) Capillary electrophoresis profile of a subset of strain-specific fragments (400–500 nt range) from marker set 8 that includes *fabF*-AS. This marker is detected by multiplex PCR in the cell lysate from mock-treated cells (highlighted in green) but not from cells treated with platensimycin (asterisk). Grey bars represent marker-specific mobility ranges recognized by the ABI Genemapper software.

(C) The completed AISS profile of platensimycin, generated from normalized data (see Experimental Procedures), includes doses from a total of five experiments. The log2 depletion ratio is shown on the y axis and represents the fold strain depletion versus DMSO mock controls. The z score denoting the significance of the depletion shown on the x axis is derived from strain-specific error models. Data points represent individual compound doses.

drug target along with an interdependent step in peptidoglycan synthesis indirectly affected by the compound's mode of action.

Unlike the above clinically used antibiotics, compound D constitutes a new predevelopment small molecule whose inhibitory effect has been linked to the largely uncharacterized gene SAV1754 (Mott et al., 2008), annotated as *SA1575* in the *S. aureus* N315 genome. Consistent with its predicted drug target, AISS profiling of compound D highlights dramatic and highly significant depletions of the SAV1754-AS strain (Figure 4D), corroborating its reported MOA. Based on highly related AISS profiles between compound D and two newly discovered bioactive compounds (DMPI and CDFI) described in an accompanying paper by Roemer and colleagues (Huber et al., 2009 [this issue of *Chemistry & Biology*]), we demonstrate by genetic means that this latter class also likely targets SAV1754 and propose that SAV1754 may function as a peptidoglycan precursor flippase.

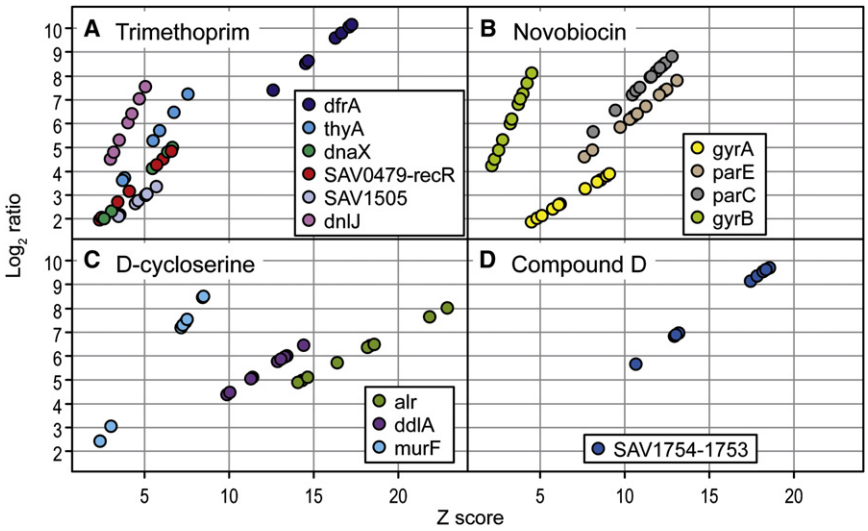

Figure 4. AISS Profiles Reflecting Selective Inhibition at Enzyme Targets

(A) trimethoprim and *dfrA*/*thyA*; (B) novobiocin and *gyrA*/*B*, *parC*/*E* (gyrase/topoisomerase); (C) D-cycloserine and *alr*/*ddlA*; (D) compound D and *SAV1754*. Data points represent independent compound doses across a minimum of two profiling experiments. Data were stringently filtered to show only strain depletions represented in >90% of the doses, with log2 ratio and z score thresholds set at 1.8 and 2.0, respectively. Additional less consistent compound-induced strain depletions are represented in Table S3 and the unfiltered average responses for the 245 strains to each of these compounds are represented in Figure S2.

Two-Dimensional Cluster Analysis of the Reference Data Set

A 2D hierarchical clustering of AISS profiles from all of the compounds and significantly depleted strains demonstrates the overall relationship between AISS profiles of compounds with either similar or diverse biological MOAs (Figure 5). The compound profiles group into four major branches (A–D), which broadly represent different modes of antibacterial action.

AISS profiles of DNA intercalators, DNA damaging agents, and inhibitors of DNA gyrase and topoisomase form the first branch of the cluster (Figure 5, group A). This branch is comprised of four major subgroups: profiles of the DNA binding drugs actinomycin D, echinomycin, and daunorubicin; the four fluoroquinolone DNA gyrase and topoisomerase IV inhibitors (ciprofloxacin, norfloxacin, nadifloxacin, and gatifloxacin); the nonenzyme-mediated DNA damaging agent streptonigrin; and the coumarin DNA gyrase and topoisomerase IV inhibitors novobiocin and coumermycin.

Actinomycin and echinomycin are structurally similar compounds that block RNA synthesis by binding to the minor groove of double stranded DNA (Sobell, 1985; Waring and Wakelin, 1974). Actinomycin can also interfere with DNA replication and has been used as an antitumor agent. Their complex but tightly clustering profiles (0.82 correlation) are characterized by common depletions in antisense strains corresponding to genes on a 29-member superoperon. These antisense strains include *adk* (adenosine kinase), *secY* (protein secretion), *rpsK*, *rplQ*, *rpsM*, *rpsE*, *rplN*, *rplP* (ribosomal proteins), *infA* (initiation factor), and *rpoA* (RNA polymerase α subunit). A possible explanation for this characteristic signature is that hypersensitivity of these strains to the DNA intercalators is a secondary consequence of antisense interference with expression of the cotranscribed *rpoA* gene (see Discussion).

Daunorubicin is an anthracycline antitumor agent that binds DNA and induces covalent interstrand DNA crosslinks leading to double strand breaks (Fukushima et al., 1993; Sartiano et al., 1979; Skladanowski and Konopa, 1994). Its profile shows some overlap with actinomycin and echinomycin, but strong uncommon depletions in *recR-AS* and *gyrB-AS* strains are also present. Depletions in the *recR* and *hu*-AS strains are shared by the nonselective DNA damaging agent streptonigrin and the fluoroquinolones, which induce double-stranded breaks through selective inhibition of topoisomerase. The *S. aureus* RecR protein is the orthologue (39% identity) of the *E. coli* RecR enzyme that is involved in recombinational DNA repair (Chow and Courcelle, 2004; Ivancic-Bace et al., 2003; Morimatsu and Kowalczykowski, 2003).

In contrast to the profiles of the four fluoroquinolone topoisomerase inhibitors, the AISS profiles of novobiocin and coumermycin show strong depletions in the *parC-AS* and *parE-AS* (topoisomerase IV subunits) strains, reflecting differences in the MOAs of these two distinct classes of topoisomerase inhibitors that are supported by a large body of molecular and biochemical evidence (reviewed in Drlica, 1999; Oblak et al., 2007). Interestingly, the representation of these strains in the AISS assay is enhanced (rather than depleted) by fluoroquinolone treatment (Figure 5, cyan-colored *parC* and *parE* tiles). By effectively reducing the level of topoisomerase, antisense expression appears to confer a fitness advantage to drug-treated cells by mitigating the associated enzyme-mediated toxicity.

Also clustering within group A is trimethoprim (see also Figure 4A) and the RNA polymerase inhibitor rifampin. The antisense strains most consistently depleted by rifampin are *sigA*-AS (RNA polymerase sigma factor) and *rpoC*-AS (RNA polymerase β' subunit), although a variety of DNA replication-associated strains are also depleted. Rifampin inhibits transcription by binding to the β subunit of the RNA polymerase core enzyme complex (reviewed in Wehrli, 1977). Structural evidence also suggests that β subunit binding by rifampin induces an allosteric change that can affect the sigma factor interaction (Artsimovitch et al., 2005).

A broad range of antibiotics compromise the peptidoglycan cell wall and underlying plasma membrane. Targets include intracellular enzymes of isoprenoid and cell wall biosynthesis, as well as transglycolases (TG) and transpeptidases (TP) located external to the plasma membrane. AISS profiles from 18 compounds that interfere diversely with the integrity of the cell wall and plasma membrane form the second major branch of

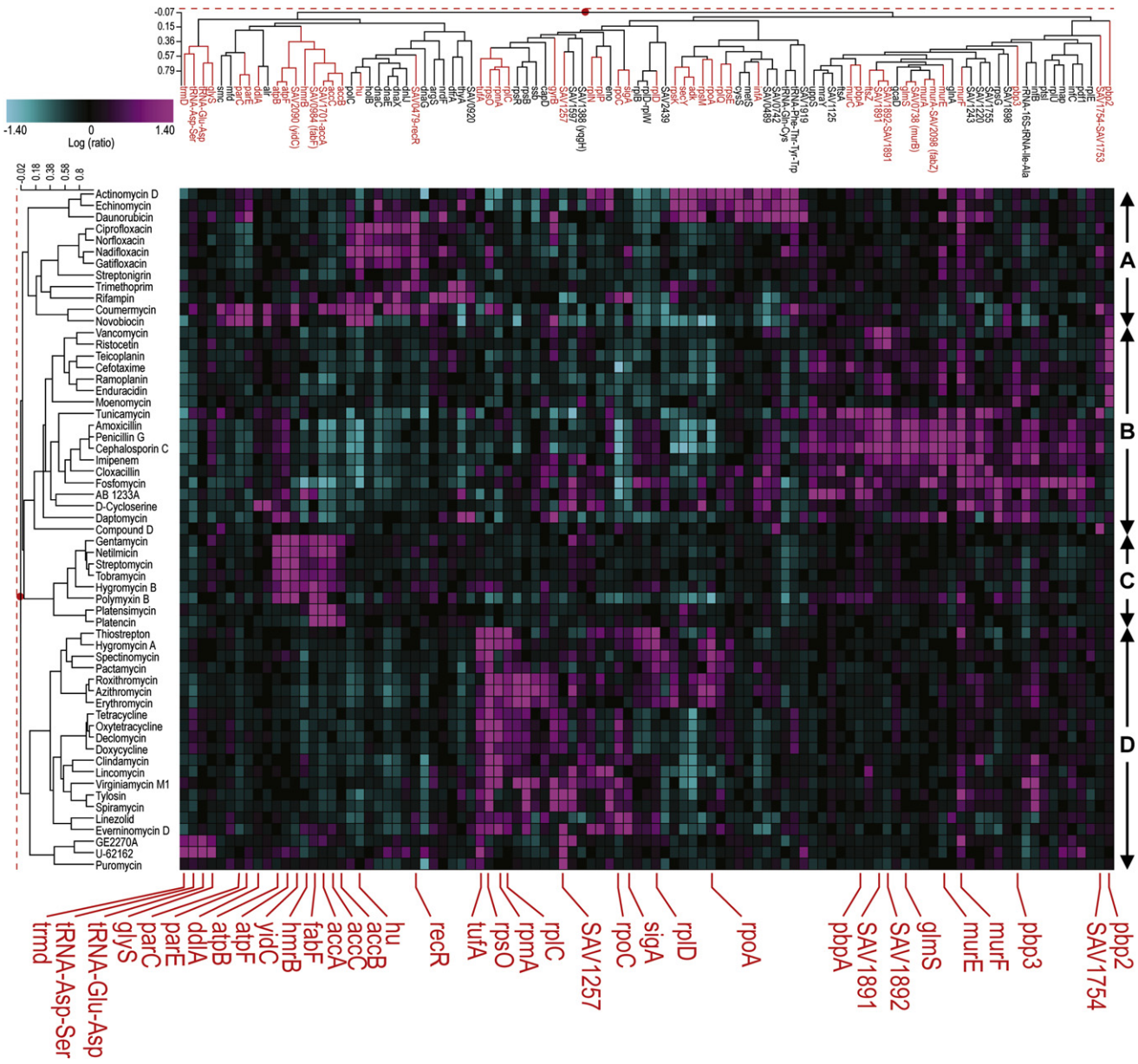

Figure 5. Two-Dimensional Cluster Analysis of AISS Profiles for 59 Antibacterial Compounds and 101 Significantly Depleted Strains

Strain depletions are depicted in magenta and strain resistances in cyan (log_{10} ratio scale). Depletion ratio and p-value data for each compound are represented as a combined profile (combo) of the set of profiles for a range of doses. The plot was generated using the Rosetta Resolver 2D cluster tool. Cluster parameters, selection of significantly depleted strains for the analysis, and the generation of combos are described in the Experimental Procedures. The compound profiles cluster into four major branches or subclusters: (A) a cluster of 12 nucleic acid synthesis/replication inhibitors; (B) a cluster of 16 cell wall biosynthesis inhibitors along with isoprenoid biosynthesis inhibitor AB1233A and membrane depolarizer daptomycin; (C) a cluster of 5 aminoglycosides along with FAS inhibitors platensimycin and platensin, and polymyxin B; and (D) a cluster of 20 protein synthesis inhibitors along with U-62162, a natural product inhibitor with an unknown MOA. Highlighted antisense strains (red) are discussed in the text.

the reference cluster (Figure 5, group B). Strong depletions in the *pbp2*-AS strain define a major subgroup of this branch that includes the profiles of TG and TP inhibitors affecting peptidoglycan assembly and crosslinking, respectively. PBP2 is an essential bifunctional enzyme of the penicillin binding protein (PBP) family, possessing separate TG and TP domains (Scheffers and Pinho, 2005). A highly correlated subgroup (0.79 correlation) includes the cephalosporin cefotaxime and the glycopeptide teicoplanin. Cefotaxime is a third generation cephalosporin of the same structural class as ceftizoxime (Greenwood et al., 1980), a highly selective inhibitor of the *S. aureus* PBP2 TP (Leski and Tomasz, 2005). Teicoplanin is a lipoglycopeptide that binds to Lipid II and inhibits the transglycosylation step of peptidoglycan synthesis (reviewed in Kahne et al.,

2005). The striking relatedness between cefotaxime and teicoplanin profiles may reflect how both agents preferentially target PBP2, albeit by mechanistically distinct means, with cefotaxime preferentially acylating the PBP2 TP active site versus teicoplanin binding to lipid II peptidoglycan precursor, which blocks substrate recognition of the PBP2 TG activity (reviewed in Ostash and Walker, 2005). Additional peptidoglycan substrate inhibitors clustering in this group are cyclic depsipeptides (enduracidin and ramoplanin) and glycopeptides (vancomycin and ristocetin), which form distinct subgroups (each with 0.76 correlation). Whereas ramoplanin was originally thought to bind Lipid I peptidoglycan substrate of MurG (Somner and Reynolds, 1990), ramoplanin and the structurally related natural product enduracidin have been shown to preferentially bind Lipid II and inhibit the TG step of peptidoglycan synthesis (Fang et al., 2006). Consistent with this revised mechanism, both compounds share a high degree of correlation between their AISS profiles and other stage III TG and TP inhibitors. Interestingly, two uncharacterized open reading frames corresponding to SAV1892 and SAV1891 are revealed in the profiles of these agents. The SAV1892 gene encodes a putative transglycosylase (COG0769M, UDP-N-acetylmuramyl tripeptide synthetase-like), while the cotranscribed SAV1891 gene encodes a poorly characterized amidotransferase (COG3442). Based on their shared hypersensitivity to these cell wall inhibitors, we speculate that SAV1892 and/or SAV1891 may directly or indirectly function in cell wall assembly. Moenomycin, a PBP2 TG inhibitor that directly binds to bacterial TG enzymes (van Heijenoort, 2001; Vogel et al., 2000), is rooted in this subgroup, largely due to the selective hypersensitivity of *pbp2*-AS.

Depletions in the *pbp2*-AS strain are completely absent from AISS profiles of β-lactams penicillin, amoxicillin, cloxacillin, imipenem, and cephalosporin C. Profiles for these compounds (0.67 correlation) form the core of the second major subgroup of the cell wall and plasma membrane branch and include depletions in additional PBP strains, *pbpA*-AS and/or *pbp3*-AS. This subgroup is further characterized by depletions of a broader range of cell wall-associated strains, including those corresponding to *glmS*, *murA*, *murB*, *murC*, *murE*, *murF*, *ftsZ*, and the previously described SAV1891/SAV1892. Similarly, the AISS profile of compound D also clusters with cell wall inhibitors, largely due to the common depletion of the SAV1754-AS strain with this agent as well as with cephalosporin C and tunicamycin treatments. However, unlike other cell wall inhibitors comprising this group, compound D appears relatively selective for the SAV1754-AS strain.

The third major branch (Figure 5, group C) of the cluster comprises bactericidal aminoglycosides such as gentamicin as well as lipid synthesis inhibitors (platensymicin and platensin) and the membrane disrupter polymyxin B. Perhaps surprisingly, these aminoglycosides form a group (root correlation value 0.74) characterized by depletions that do not reflect inhibition of ribosomal protein synthesis. Prominent are depletions of strains associated with fatty acid biosynthesis (*hmrB*, *fabF*, and *accA/B/C*), ATP synthase (*atpB/F*), and protein translocation (*yidC*). Although aminoglycosides bind to the ribosome and inhibit protein synthesis, the cytocidal effects of aminoglycosides cannot be explained by inhibition of protein synthesis alone (reviewed in Hancock, 1981a, 1981b). Moreover, the lack of a protein synthesis inhibition signature within their AISS profile does not reflect technical limitations associated with antisense interference of genes participating in ribosome and/or translation processes, as such elements are highly sensitive to other classes of protein synthesis inhibitors, including the bacteriostatic aminoglycoside spectinomycin (see below). Instead, AISS profiles are consistent with the hypothesis that the cytocidality of these aminoglycosides involves (in part) compromising the integrity of the plasma membrane by mistranslation of membrane proteins, as recently reported (Kohanski et al., 2008).

The fourth major branch of the compendium cluster (Figure 5, group D) contains 20 protein synthesis inhibitors and one antibacterial of unknown MOA. The most hypersensitive and frequently depleted antisense strain in this set of compounds is *rpsO*-AS. The *rpsO* gene encodes ribosomal protein S15, which is highly conserved among prokaryotes and is thought to play a role in ribosome assembly (Culver et al., 1999; Held et al., 1974). Immediately apparent from the hierarchical clustering is the resolution of compounds into discrete subgroups, some according to antibiotic structure and/or MOA. The first subgroup characterized by *rpsO*-AS depletions contains four structurally unrelated compounds (thiostrepton, hygromycinA, spectinomycin, and pactamaycin) with different mechanisms of ribosome binding (Bowen et al., 2005; Guerrero and Modolell, 1980; Wirmer and Westhof, 2006). The AISS profiles for these compounds share additional depletions of *tufA*-AS, *rplD*-AS, and *rpoA*-AS. The macrolides are divided into two distinct but structurally related subgroups. Tylosin and spiramycin (0.90 correlation) contain a disaccharide at position 5 in the lactone ring with a mycarose moiety that seems to be correlated with inhibition of peptidyl transferase (Poulsen et al., 2000). Erythromycin, azithromycin, and roxithromycin, which lack this moiety and functional capability, form a separate subgroup (0.90 correlation). Four tetracycline compounds cluster tightly together (0.92 correlation) and show depletions of a variety of translation-associated strains, including *rpsO*-AS, *rpmA*-AS, *rplC*-AS, *tufA*-AS (EF-Tu), and SAV1257-AS (EF-Ts).

Depletions of *rpsO*-AS are noticeably absent from the profiles of GE2270A and puromycin. The profiles of these similarly clustering compounds (0.64 correlation) share common depletions of *tufA*-AS and SAV1257-AS (elongation factors Tu and Ts). GE2270A binds to EF-Tu and inhibits its interaction with aminoacylated tRNAs (Parmeggiani and Nissen, 2006; Selva et al., 1991). Puromycin is an aminoacylated tRNA analogue that is incorporated into the nascent polypeptide, but blocks elongation due to the resulting nonhydrolysable amide bond (Azzam and Algranat, 1973). Interestingly, the antibiotic U-62162, an epoxide of the manumycin family with unknown MOA (Slechta et al., 1982), clusters with GE2270A. In addition to depletions in the elongation factor antisense strains, tRNA-associated strains *trmD*-AS, *glyS*-AS, and *tRNAGlu/Asp/Ser*-AS are also hypersensitive to both compounds.

DISCUSSION

Here we describe the successful adaptation of the fitness test approach for compound MOA determination in the clinically important bacterial pathogen *S. aureus*. Although the basic concept of a collection of target-depleted, sensitized strains

grown in a competitive fitness test is analogous to yeast-based systems, the underlying technologies are different. The fungal platforms rely on comprehensive genome-wide sets of heterozygote strains and a DNA chip-based detection system. The analogous *S. aureus* platform utilizes a smaller collection of 245 antisense sensitized strains representing a subset of genes that are essential for growth and uses a capillary electrophoresis-based detection system. In this case, effective titration of antisense expression by xylose inducer can range from a conditional knockout phenotype to a more modest level of growth suppression (~20%) that maximizes target-based sensitivity for the fitness test experiment. The key to success of this approach is the pooling of strains into bins based on their xylose sensitivities allowing for a competitive growth experiment to be performed while maintaining appropriate target-depleted sensitization for the essential gene targets represented in the array.

Through profiling of a diverse set of antibiotics (n = 59) with this novel platform we have generated a reference set of AISS profiles that allows us to recognize signatures reflecting antibacterial mechanisms at established drug targets. These targets include metabolic enzymes as well as multienzyme complexes involved in ribosomal translation, cell wall biosynthesis, and DNA replication. Compound MOA can either be inferred directly from AISS profiles or from pattern matching in 2D clustering to the AISS profiles of compounds with defined MOAs. The clustering of antibiotic U62162 with elongation inhibitor GE2270A suggests a common mechanism (Figure 5). Much as the ''compendium'' approach has proved a powerful tool for elucidating compound MOAs from gene expression profiles and chemical genetic profiles from a yeast haploid deletion set (Hughes et al., 2000; Parsons et al., 2006), such a reference data set-based approach allows us to infer a biological MOA for U-62162. Although this hypothesis requires further investigation, metabolic labeling experiments (not presented) show that the compound is indeed a selective inhibitor of translation but not of nucleic acid, cell wall, or fatty acid biosynthesis.

The AISS profile data set presented here provides insights into the whole-cell MOAs of a wide range of antibiotics along with information about gene function, some of which are highlighted in this report. Prominent in the AISS cluster analysis of inhibitors of translation and cell wall/membrane (Figure 5) are a limited number of antisense strains that deplete across specific subgroups. For the ribosomal antibiotics, all but the classic aminoglycosides and a pair of elongation inhibitors (GE2270A and puromycin) show depletions in the *rpsO*-AS (ribosomal protein S15) strain. For cell wall inhibitors, depletions in the *pbp2*-AS strain appear to define a group of putative TP and TG inhibitors that cluster distinctly from the major group of β-lactams, including bona fide inhibitors of PBP2 TP or TG. While these strains can serve as beacons of specific biological responses in an AISS profile, they can also be adapted for use as individual whole cell screens for the detection of target- and pathway-specific antibiotics.

Notwithstanding the clear advantages AISS profiling provides in determining the MOA of antibiotics, it does possess some limitations. For example, the platform has been purposely biased to represent genes essential for growth under laboratory conditions; nonessential cellular processes that contribute to pathogenesis including virulence factors and antibiotic resistance determinants have so far been excluded from study. Ionophores with antibacterial activity, such as monensin and nigericin, and the protonophore tetrachlorosalicylanilide fail to generate mechanistically informative AISS profiles (not presented). This may reflect limitations of genome coverage in the current strain set or the inability to detect such MOAs through the fitness test approach. The discriminating power of the array is likely to be enhanced by the inclusion of antisense strains or loss-of-function mutants corresponding to nonessential genes encoding transcriptional regulators, efflux pumps, or virulence factors that can influence susceptibility to particular antibiotics.

Biological constraints are also imposed on fitness test screening within a bacterial pathogen. Unlike in eukaryotes, gene operons and polycistronic transcripts can complicate genetic depletion of individual targets by antisense interference or other genetic means. Consequently, linking a compound to its cognate target may not be as straightforward in instances where antisense-induced strain depletions result from individual antisense fragments targeting either a polycistronic message (the most dramatic being the 29 member superoperon effected by actinomycin and echinomycin) or two adjacent open reading frames, as in the case of SAV1891-SAV1892-AS and SAV1754-SAV1753-AS strains. Interestingly, although *ddlA* and *murF* are cotranscribed, gene-specific antisense interference of these targets produces specific strain hypersensitivities: D-cycloserine specifically affects *ddlA*-AS and *murF*-AS strain depletions, whereas other cell wall inhibitors broadly affect *murF*-AS but not the *ddlA*-AS strain. Complex AISS profiles may also result for compounds with MOAs associated with a single drug target. For example β-lactam antibiotics specifically inhibit bacterial growth by acylating essential PBPs. However, AISS profiles capture not only their drug target (e.g., PBPA, PBP2, and/or PBP3, depending on the β-lactam) but also multiple additional steps in peptidoglycan biosynthesis, which if impaired sensitize *S. aureus* to these agents. Thus, the biological relevance of such profiles not only underscores the general process affected by β-lactams, namely cell wall assembly, but also provides important clues as to subtle differences in biological MOA and potential interactions between the drug target and other cellular components.

Importantly, AISS profiling serves as a valuable MOA hypothesis tool for characterizing new bioactive compounds. However, additional genetic and/or biochemical evidence is required to test such hypotheses. Indeed, in the accompanying paper by Roemer and colleagues in this issue of *Chemistry & Biology*, we demonstrate how AISS profiling of new synthetic antibacterial compounds is used to guide genetic, biochemical, and cell biological-based secondary assays and establish their likely drug target, SAV1754, a previously uncharacterized cell surface transmembrane protein involved in cell wall assembly (Huber et al., 2009). Thus, the timely extension of fitness test profiling tools for MOA determination in the bacterial pathogen *S. aureus* should provide an important chemical genetic strategy to benefit many aspects of antibacterial drug discovery.

SIGNIFICANCE

The search for new lead molecules in antibacterial drug discovery is a daunting task that is complicated by the fact

that a large percentage of the small molecules in synthetic or natural product libraries have some level of intrinsic antibacterial activity. Establishing which of these molecules might be working through an attractive target-based mechanism and prioritizing them for lead optimization chemistry efforts represents a significant bottleneck in the discovery process. Based on an array of 245 target-depleted antisense strains corresponding to essential genes, the *S. aureus* antisense platform described in this paper offers a solution by yielding reproducible information-rich profiles that reflect a compound's biological mechanism. As demonstrated with a diverse set of reference antibiotics, inhibition of single enzyme targets or multienzyme complexes can be reliably and rapidly detected. The inclusion in the array of antisense strains corresponding to uncharacterized *S. aureus* essential genes facilitates the identification of compounds inhibiting growth through novel mechanisms (e.g., compound D; Mott et al., 2008). In practice, this platform has utility as a cell-based target selectivity assay to guide antibiotic medicinal chemistry and natural product isolation chemistry efforts. In addition, the underlying concepts of strain binning, strain detection, and data analysis have potentially broader application to other pathogens or model systems where stable RNA interference technologies have been established.

EXPERIMENTAL PROCEDURES

Plasmids and Strains

S. aureus strain RN4220 was used as host for all antisense plasmids (Novick, 1991). For new antisense vector construction, inverted gene fragments (200–300 bp) spanning the target gene were subcloned into pEPSA5 vector BamHI and SmaI sites (Forsyth et al., 2002) using standard techniques. Representative clones harboring gene fragments conferring the strongest conditional growth phenotype in *S. aureus* were selected for the array. Antisense plasmids were introduced into RN4220 by electroporation (Kraemer and Iandolo, 1990) and stable transformants were selected on LB chloramphenicol agar plates (34 μg/ml). Gene annotation of the antisense strain set is based on the *S. aureus* Mu50 genome (Kuroda et al., 2001), which is predicted to encode 864 monocistronic transcripts and 533 polycistronic operons (Wang et al., 2004). The antisense strains described in this work (Table S1) are available for noncommercial use following the standard Merck Material Transfer Agreement and clearance procedures.

Xylose Titrations and Binning of Strains

Growth media used for all experiments was prepared from Miller's Luria broth base (single lot; Invitrogen), filter sterilized (0.22 μM membrane; Millipore), and supplemented with 34 μg/ml chloramphenicol for maintenance of antisense plasmids (Sigma). Individual *S. aureus* antisense strains were grown independently over three cycles (see Supplemental Experimental Procedures) in the presence of xylose ranging from 0 to 100 mM generating dose response curves with varying IC_{50} values, slopes, and minima. Strains were ordered by IC_{20} values calculated using the values from the end of the third cycle and were grouped into bins by ensuring an overlap of the IC_{10} and IC_{30} of neighboring strains and targeting an optimum of ten strains per bin (Table S1). Some manual adjustments were made to bin composition based on empiric observations and previous strain performance in early prototype versions of the profiling platform. Xylose concentrations for each individual bin were determined by averaging the IC_{10} values for all strains represented in the bin. This resulted in 24 unique bins having 6–12 strains per bin with xylose concentrations for the entire array ranging from 1.8-55 mM. In this bin configuration two antisense strains, AS-169 (SAV1901-SAV1900) and AS-302 (SAV1113-ylaO), were eliminated from all experiments because of poor peak area signal in the DMSO mock treatment controls.

Platform Instrumentation

The fully automated assay system for processing 384 well growth plates through three cycles of growth consisted of a Tecan Genesis (or Evo) with a ROMA for plate handling, a Hereaus Cytomat 6000 for plate incubation, a Biotek PowerWaveHT for cell growth end point determination, and a Matrix PlateMate 2 × 2 for back dilutions. One experimental unit for this platform is defined as six initial 384 well growth plates containing a total of 12 different compounds each dosed at six different concentrations and 12 DMSO mock treatment controls. Instruments and scheduling were controlled through Tecan's FACTS software with custom integration code for nonstandard instruments. Matrix PlateMatePlus instruments were used to process microplates for microbiology and molecular biology steps (details in Supplemental Experimental Procedures). An ABI9700 Dual 384 well thermocycler was used for multiplex PCR and products were analyzed on an ABI3730 genetic analyzer.

Oligonucleotide Markers and Multiplex PCR Primer Sets

Strain-specific oligonucleotides (IDT) and the antisense plasmid inserts to which they selectively anneal are described in Table S7. The makers include a synthetic 5′ 7 bp extension (GTTTCTT) to improve multiplex PCR efficiency. The primers (T_m 48–52°C, minus extension) were designed to generate fragments in the 200 to 500 nt range when used in combination with an anchored VIC-labeled vector primer (common to all plasmids) that anneals to the proximal xylose promoter (5′VIC-CAGCAGTCTGAGTTATAAAATAG, synthesized by ABI). Performance of individual primers was initially optimized in PCR reactions with mock cell lysates (all strains as template) to eliminate those yielding secondary products (in singleplex PCR) or poor signal (in multiplex PCR). Validated primers were organized into eight multiplex sets of 30–32 that yield well-spaced (≥4 nt gap) strain-specific PCR fragments readily resolvable by ABI3730 capillary electrophoresis with ABI Genemapper software.

Data Normalization, Statistical, and Cluster Analysis

Individual variability of an oligonucleotide marker was normalized by calculating the marker's area as a percentage of total composite signal for its particular multiplex marker set ($\%p_i = p_i / \sum p_n$). Subsequently, the strain depletion ratio was calculated as a $\log_{10}$ of the median DMSO control percent area (calculated from the entire set of data from one experimental unit; see Platform Instrumentation section) divided by the individual strain percent area ($R_i = \log_{10}(median(\%C)/\%p_i)$). This approach required defining a minimum background value for potential fully depleted strains. Statistical significance was determined as a p-value utilizing an error model generated for each individual strain across a discrete set of known standards and unknown test samples selected to represent total coverage of all strains within the array set. Z score or Xdev was calculated as $\log_{10}$ depletion ratio minus the median $\log_{10}$ depletion ratio for the error model divided by the median absolute deviation ($Xdev = (R_i - median(R_c))/median(|R_i - median(R_c)|)$). P-value was then calculated as the standard complementary error function ($p - value = erfc(|Xdev/\sqrt{2}|)$. Calculated $\log_{10}$ depletions and corresponding p-values were then loaded into Rosetta Resolver as Ratio Experiments for subsequent cluster analysis. Reference compound profiles were then represented in Resolver as combos in which several (4–10) appropriately dosed representative experiments were combined into one and the $\log_{10}$ ratio calculated as an error-weighted mean of the $\log_{10}$ ratio from each experiment. The combined $\log_{10}$ ratio error was calculated as a blend of two error components, the "propagated" error and the "scattered" error. The propagated error is the average of the $\log_{10}$ ratio divided by square root of the number of experiments ($p = 1/n \sum_{i=1}^{n} R_i/\sqrt{n}$) and the scattered error (s) is an error-weighted standard deviation of the profile $\log_{10}$ ratio values. The blend of the two components is a linear blending where $\log_{10}$ ratio error $= p/n + (s(n-1)/1)$. Thus the combined $\log_{10}$ ratio error equals the propagated error if n = 1 but the dominant contributor is the scattered error as n increases. Two-dimensional cluster analysis was performed on the combined experiments (combos) in Rosetta Resolver utilizing an agglomerative algorithm with average link heuristic criteria and a cosine correlation similarity measure. The antisense strains used for the clustering exercise were selected if they were significantly depleted in the profiles for those compound treatments making up a given combo experiment. The thresholds set for determining strain significance for each set of compound profiles were at least a 5-fold depletion and p-value ≤0.01 in at least 75% of the experiments making up the combo for the given compound.

Once significantly depleted strains were identified for each of the compounds in this way they were then added to a Resolver sequence set that was used to build the 2D cluster shown in Figure 5.

SUPPLEMENTAL DATA

Supplemental Data include Supplemental Experimental Procedures, two figures, and seven tables and can be found with this article online at http://www.cell.com/chemistry-biology/supplemental/S1074-5521(09)00214-2.

ACKNOWLEDGMENTS

We thank Michael Goetz, Sheo Singh, and Ken Wilson for providing natural product reference compounds. We also acknowledge the efforts of scientists at Elitra Pharmaceuticals who laid the foundation for this work and colleagues Terry Roemer and David Pompliano for reviewing the manuscript. Some of the authors are employees of Merck & Co., Inc., as stated in the affiliations, and potentially own stock and/or hold stock options in the Company.

Received: March 6, 2009
Revised: May 25, 2009
Accepted: July 9, 2009
Published: August 27, 2009

REFERENCES

Artsimovitch, I., Vassylyeva, M.N., Svetlov, D., Svetlov, V., Perederina, A., Igarashi, N., Matsugaki, N., Wakatsuki, S., Tahirov, T.H., and Vassylyev, D.G. (2005). Allosteric modulation of the RNA polymerase catalytic reaction is an essential component of transcription control by rifamycins. Cell *122*, 351–363.

Azzam, M.E., and Algranat, I.D. (1973). Mechanism of puromycin action: fate of ribosomes after release of nascent protein chains from polysomes. Proc. Natl. Acad. Sci. USA *70*, 3866–3869.

Baetz, K., McHardy, L., Gable, K., Tarling, T., Reberioux, D., Bryan, J., Andersen, R.J., Dunn, T., Hieter, P., and Roberge, M. (2004). Yeast genome-wide drug-induced haploinsufficiency screen to determine drug mode of action. Proc. Natl. Acad. Sci. USA *101*, 4525–4530.

Bellon, S., Parsons, J.D., Wei, Y.Y., Hayakawa, K., Swenson, L.L., Charifson, P.S., Lippke, J.A., Aldape, R., and Gross, C.H. (2004). Crystal structures of *Escherichia coli* topoisomerase IV ParE subunit (24 and 43 kilodaltons): a single residue dictates differences in novobiocin potency against topoisomerase IV and DNA gyrase. Antimicrob. Agents Chemother. *48*, 1856–1864.

Bowen, W.S., Van Dyke, N., Murgola, E.J., Lodmell, J.S., and Hill, W.E. (2005). Interaction of thiostrepton and elongation factor-G with the ribosomal protein L11-binding domain. J. Biol. Chem. *280*, 2934–2943.

Burchall, J.J. (1973). Mechanism of action of trimethoprim-sulfamethoxazole. II. J. Infect. Dis. *128* (*Suppl*), 437–441.

Chow, K.H., and Courcelle, J. (2004). RecO acts with RecF and RecR to protect and maintain replication forks blocked by UV-induced DNA damage in *Escherichia coli*. J. Biol. Chem. *279*, 3492–3496.

Culver, G.M., Cate, J.H., Yusupova, G.Z., Yusupov, M.M., and Noller, H.F. (1999). Identification of an RNA-protein bridge spanning the ribosomal subunit interface. Science *285*, 2133–2135.

DeVito, J.A., Mills, J.A., Liu, V.G., Agarwal, A., Sizemore, C.F., Yao, Z., Stoughton, D.M., Cappiello, M.G., Barbosa, M.D.F.S., Foster, L.A., et al. (2002). An array of target-specific screening strains for antibacterial discovery. Nat. Biotechnol. *20*, 478–483.

Drlica, K. (1999). Mechanism of fluoroquinolone action. Curr. Opin. Microbiol. *2*, 504–508.

Fang, X., Tiyanont, K., Zhang, Y., Wanner, J., Boger, D., and Walker, S. (2006). The mechanism of action of ramoplanin and enduracidin. Mol. Biosyst. *2*, 69–76.

Feng, Z., and Barletta, R.G. (2003). Roles of *Mycobacterium smegmatis* D-alanine:D-alanine ligase and D-alanine racemase in the mechanisms of action of and resistance to the peptidoglycan inhibitor D-cycloserine. Antimicrob. Agents Chemother. *47*, 283–291.

Forsyth, R.A., Haselbeck, R.J., Ohlsen, K.L., Yamamoto, R.T., Xu, H., Trawick, J.D., Wall, D., Wang, L., Brown-Driver, V., Froelich, J.M., et al. (2002). A genome-wide strategy for the identification of essential genes in *Staphylococcus aureus*. Mol. Microbiol. *43*, 1387–1400.

Fujimoto-Nakamura, M., Ito, H., Oyamada, Y., Nishino, T., and Yamagishi, J. (2005). Accumulation of mutations in both gyrB and parE genes is associated with high-level resistance to novobiocin in *Staphylococcus aureus*. Antimicrob. Agents Chemother. *49*, 3810–3815.

Fukushima, T., Ueda, T., Uchida, M., and Nakamura, T. (1993). Action mechanism of idarubicin (4-demethoxydaunorubicin) as compared with daunorubicin in leukemic cells. Int. J. Hematol. *57*, 121–130.

Giaever, G., Shoemaker, D.D., Jones, T.W., Liang, H., Winzeler, E.A., Astromoff, A., and Davis, R.W. (1999). Genomic profiling of drug sensitivities via induced haploinsufficiency. Nat. Genet. *21*, 278–283.

Giaever, G., Flaherty, P., Kumm, J., Proctor, M., Nislow, C., Jaramillo, D.F., Chu, A.M., Jordan, M.I., Arkin, A.P., and Davis, R.W. (2004). Chemogenomic profiling: identifying the functional interactions of small molecules in yeast. Proc. Natl. Acad. Sci. USA *101*, 793–798.

Greenwood, D., Pearson, N., Eley, A., and Ogrady, F. (1980). Comparative in vitro activities of cefotaxime and ceftizoxime (fk749)–new cephalosporins with exceptional potency. Antimicrob. Agents Chemother. *17*, 397–401.

Guerrero, M.D., and Modolell, J. (1980). Hygromycin A, a novel inhibitor of ribosomal peptidyltransferase. Eur. J. Biochem. *107*, 409–414.

Hancock, R.E.W. (1981a). Aminoglycoside uptake and mode of action-with special reference to streptomycin and gentamicin. 2. Eeffects of aminoglycosides on cells. J. Antimicrob. Chemother. *8*, 429–445.

Hancock, R.E.W. (1981b). Aminoglycoside uptake and mode of action with special reference to streptomycin and gentamicin. 1. Antagonists and mutants. J. Antimicrob. Chemother. *8*, 249–276.

Held, W.A., Ballou, B., Mizushim, S., and Nomura, M. (1974). Assembly mapping of 30 S ribosomal proteins from *Escherichia coli*. Further studies. J. Biol. Chem. *249*, 3103–3111.

Hitchings, G.H. (1973). Mechanism of action of trimethoprim-sulfamethoxazole. I. J. Infect. Dis. *128*, 433–436.

Huber, J., Donald, R.G.K., Lee, S.H., Wang Jarantow, L., Salvatore, M.J., Meng, X., Painter, R., Onishi, R., Occi, J., Dorso, K., et al. (2009). Chemical genetic identification of peptidoglycan inhibitors that potentiate carbapenem activity against methicillin-resistant *Staphylococcus aureus*. Chem. Biol. *16*, this issue, 837–848.

Hughes, T.R., Marton, M.J., Jones, A.R., Roberts, C.J., Stoughton, R., Armour, C.D., Bennett, H.A., Coffey, E., Dai, H., He, Y.D., et al. (2000). Functional discovery via a compendium of expression profiles. Cell *102*, 109–126.

Ivancic-Bace, I., Peharec, P., Moslavac, S., Skrobot, N., Salaj-Smic, E., and Brcic-Kostic, K. (2003). RecFOR function is required for DNA repair and recombination in a RecA loading-deficient recB mutant of *Escherichia coli*. Genetics *163*, 485–494.

Ji, Y., Zhang, B., Van Horn, S.F., Warren, P., Woodnutt, G., Burnham, M.K., and Rosenberg, M. (2001). Identification of critical staphylococcal genes using conditional phenotypes generated by antisense RNA. Science *293*, 2266–2269.

Jiang, B., Xu, D.M., Allocco, J., Parish, C., Davison, J., Veillette, K., Sillaots, S., Hu, W.Q., Rodriguez-Suarez, R., Trosok, S., et al. (2008). PAP inhibitor with in vivo efficacy identified by *Candida albicans* genetic profiling of natural products. Chem. Biol. *15*, 363–374.

Kahne, D., Leimkuhler, C., Lu, W., and Walsh, C. (2005). Glycopeptide and lipoglycopeptide antibiotics. Chem. Rev. *105*, 425–448.

Kamashev, D., Balandina, A., Mazur, A.K., Arimondo, P.B., and Rouviere-Yaniv, J. (2008). HU binds and folds single-stranded DNA. Nucleic Acids Res. *36*, 1026–1036.

Kohanski, M.A., Dwyer, D.J., Wierzbowski, J., Cottarel, G., and Collins, J.J. (2008). Mistranslation of membrane proteins and two-component system activation trigger antibiotic-mediated cell death. Cell *135*, 679–690.

Kraemer, G.R., and Iandolo, J.J. (1990). High-frequency transformation of *Staphylococcus aureus* by electroporation. Curr. Microbiol. *21*, 373–376.

Kuroda, M., Ohta, T., Uchiyama, I., Baba, T., Yuzawa, H., Kobayashi, I., Cui, L.Z., Oguchi, A., Aoki, K., Nagai, Y., et al. (2001). Whole genome sequencing of meticillin-resistant *Staphylococcus aureus*. Lancet *357*, 1225–1240.

Lambert, M.P., and Neuhaus, F.C. (1972). Mechanism of D-cycloserine action: alanine racemase from *Escherichia coli* W. J. Bacteriol. *110*, 978–987.

Leski, T.A., and Tomasz, A. (2005). Role of penicillin-binding protein 2 (PBP2) in the antibiotic susceptibility and cell wall cross-linking of *Staphylococcus aureus*: evidence for the cooperative functioning of PBP2, PBP4, and PBP2A. J. Bacteriol. *187*, 1815–1824.

Lum, P.Y., Armour, C.D., Stepaniants, S.B., Cavet, G., Wolf, M.K., Butler, J.S., Hinshaw, J.C., Garnier, P., Prestwich, G.D., Leonardson, A., et al. (2004). Discovering modes of action for therapeutic compounds using a genome-wide screen of yeast heterozygotes. Cell *116*, 121–137.

Morimatsu, K., and Kowalczykowski, S.C. (2003). RecFOR proteins load RecA protein onto gapped DNA to accelerate DNA strand exchange: a universal step of recombinational repair. Mol. Cell *11*, 1337–1347.

Mott, J.E., Shaw, B.A., Smith, J.F., Bonin, P.D., Romero, D.L., Marotti, K.R., and Miller, A.A. (2008). Resistance mapping and mode of action of a novel class of antibacterial anthranilic acids: evidence for disruption of cell wall biosynthesis. J. Antimicrob. Chemother. *62*, 720–729.

Novick, R.P. (1991). Genetic systems in staphylococci. Methods Enzymol. *204*, 587–636.

Oblak, M., Kotnik, M., and Solmajer, T. (2007). Discovery and development of ATPase inhibitors of DNA gyrase as antibacterial agents. Curr. Med. Chem. *14*, 2033–2047.

Ostash, B., and Walker, S. (2005). Bacterial transglycosylase inhibitors. Curr. Opin. Chem. Biol. *9*, 459–466.

Parmeggiani, A., and Nissen, P. (2006). Elongation factor Tu-targeted antibiotics: four different structures, two mechanisms of action. FEBS Lett. *580*, 4576–4581.

Parsons, A.B., Lopez, A., Givoni, I.E., Williams, D.E., Gray, C.A., Porter, J., Chua, G., Sopko, R., Brost, R.L., Ho, C.H., et al. (2006). Exploring the mode-of-action of bioactive compounds by chemical-genetic profiling in yeast. Cell *126*, 611–625.

Payne, D.J., Gwynn, M.N., Holmes, D.J., and Pompliano, D.L. (2007). Drugs for bad bugs: confronting the challenges of antibacterial discovery. Nat. Rev. Drug Discov. *6*, 29–40.

Poulsen, S.M., Kofoed, C., and Vester, B. (2000). Inhibition of the ribosomal peptidyl transferase reaction by the mycarose moiety of the antibiotics carbomycin, spiramycin and tylosin. J. Mol. Biol. *304*, 471–481.

Rodriguez-Suarez, R., Xu, D.M., Veillette, K., Davison, J., Sillaots, S., Kauffman, S., Hu, W.Q., Bowman, J., Martel, N., Trosok, S., et al. (2007). Mechanism-of-action determination of GMP synthase inhibitors and target validation in *Candida albicans* and *Aspergillus fumigatus*. Chem. Biol. *14*, 1163–1175.

Sartiano, G.P., Lynch, W.E., and Bullington, W.D. (1979). Mechanism of action of the anthracycline anti-tumor antibiotics, doxorubicin, daunomycin and rubidazone: preferential inhibition of DNA polymerase alpha. J. Antibiot. (Tokyo) *32*, 1038–1045.

Scheffers, D.-J., and Pinho, M.G. (2005). Bacterial cell wall synthesis: new insights from localization studies. Microbiol. Mol. Biol. Rev. *69*, 585–607.

Selva, E., Beretta, G., Montanini, N., Saddler, G.S., Gastaldo, L., Ferrari, P., Lorenzetti, R., Landini, P., Ripamonti, F., Goldstein, B.P., et al. (1991). Antibiotic GE2270 a: a novel inhibitor of bacterial protein synthesis. I. Isolation and characterization. J. Antibiot. (Tokyo) *44*, 693–701.

Skladanowski, A., and Konopa, J. (1994). Interstrand DNA crosslinking induced by anthracyclines in tumour cells. Biochem. Pharmacol. *47*, 2269–2278.

Slechta, L., Cialdella, J.I., Mizsak, S.A., and Hoeksema, H. (1982). Isolation and characterization of a new antibiotic U-62162. J. Antibiot. (Tokyo) *35*, 556–560.

Sobell, H.M. (1985). Actinomycin and DNA transcription. Proc. Natl. Acad. Sci. USA *82*, 5328–5331.

Somner, E.A., and Reynolds, P.E. (1990). Inhibition of peptidoglycan biosynthesis by ramoplanin. Antimicrob. Agents Chemother. *34*, 413–419.

Taubes, G. (2008). The bacteria fight back. Science *321*, 356–361.

van Heijenoort, J. (2001). Formation of the glycan chains in the synthesis of bacterial peptidoglycan. Glycobiology *11*, 25R–36R.

Vogel, S., Buchynskyy, A., Stembera, K., Richter, K., Hennig, L., Muller, D., Welzel, P., Maquin, F., Bonhomme, C., and Lampilas, M. (2000). Some selective reactions of moenomycin A. Bioorg. Med. Chem. Lett. *10*, 1963–1965.

Wang, J., Soisson, S.M., Young, K., Shoop, W., Kodali, S., Galgoci, A., Painter, R., Parthasarathy, G., Tang, Y.S., Cummings, R., et al. (2006). Platensimycin is a selective FabF inhibitor with potent antibiotic properties. Nature *441*, 358–361.

Wang, L., Trawick, J.D., Yamamoto, R., and Zamudio, C. (2004). Genome-wide operon prediction in *Staphylococcus aureus*. Nucleic Acids Res. *32*, 3689–3702.

Waring, M.J., and Wakelin, L.P.G. (1974). Echinomycin: bifunctional intercalating antibiotic. Nature *252*, 653–657.

Wehrli, W. (1977). Ansamycins. Chemistry, biosynthesis and biological activity. Top. Curr. Chem. *72*, 21–49.

Wirmer, J., and Westhof, E. (2006). Molecular contacts between antibiotics and the 30S ribosomal particle. Methods Enzymol. *415*, 180–202.

Xu, D., Jiang, B., Ketela, T., Lemieux, S., Veillette, K., Martel, N., Davison, J., Sillaots, S., Trosok, S., Bachewich, C., et al. (2007). Genome-wide fitness test and mechanism-of-action studies of inhibitory compounds in *Candida albicans*. PLoS Pathog. *3*, e92.

Yin, D., Fox, B., Lonetto, M.L., Etherton, M.R., Payne, D.J., Holmes, D.J., Rosenberg, M., and Ji, Y. (2004). Identification of antimicrobial targets using a comprehensive genomic approach. Pharmacogenomics *5*, 101–113.

Young, K., Jayasuriya, H., Ondeyka, J.G., Herath, K., Zhang, C., Kodali, S., Galgoci, A., Painter, R., Brown-Driver, V., Yamamoto, R., et al. (2006). Discovery of FabH/FabF inhibitors from natural products. Antimicrob. Agents Chemother. *50*, 519–526.

